

See discussions, stats, and author profiles for this publication at: <https://www.researchgate.net/publication/344364677>

# A Dual Band Star-Shaped Fractal Slot Antenna: Design and Measurement

Article in *AEU - International Journal of Electronics and Communications* · September 2020

DOI: 10.1016/j.aeue.2020.153473

CITATIONS

0

READS

28

3 authors, including:



**Ra'ed A. Malallah**  
University College Dublin

44 PUBLICATIONS 133 CITATIONS

[SEE PROFILE](#)



**Wa'il A. Godaymi Al-Tumah**  
University of Basrah

43 PUBLICATIONS 21 CITATIONS

[SEE PROFILE](#)

Some of the authors of this publication are also working on these related projects:



neuroscience [View project](#)



Biophysics [View project](#)



Regular paper

## A dual band star-shaped fractal slot antenna: Design and measurement

Ra'ed Malallah<sup>\*</sup>, Raed M. Shaaban, Wa'il A. Godaymi Al-Tumah

Department of Physics, Faculty of Science, University of Basrah, Garmat Ali, Basrah, Iraq

### ARTICLE INFO

#### Keywords:

Fractal antenna  
Microstrip antenna  
Multiband  
Dual band

### ABSTRACT

In this study a new structure of a star-shaped fractal antenna was designed, simulated and fabricated, to operate at dual band applications. The geometrical of this antenna begins from two conducting squares shape to create an eight-shaped star. Added to that, the fractal geometry slot has been designed using four squares rotating in four angles to forming sixteen triangular slots. Whereas semi-circle slot shaped has been loaded in the center of the proposed antenna. The suggested antenna was designed and simulated using an Ansoft High Frequency Structure Simulator (HFSS). A few parameters such as return loss, input impedance, and radiation patterns were studying. It is found that the fabricated antenna has a dual band at two resonance frequencies 1.3308 GHz and 2.6992 GHz. The first band is used in the aviation service. While, the second band is used in the space research services, radio astronomy, and earth exploration-satellite. These dual band meets the applications in L- and S-band respectively. The simulated and measured results for return loss of the designed antenna are in a good agreement. Also, the measured and simulated values of the impedance bandwidth of the proposed antenna are (2.31% and 3.62%) and (2.57% and 3.32%), respectively. Interestingly, the semi-circle slot dimensions have significant effect on the simulation results of return loss and antenna efficiency.

### 1. Introduction

In the modern communication system, the booming technology of wireless communication is playing an essential part. The worth of a communication system depends on the proper design of the antenna. The flourishing request of wireless technology increased, therefore the features of antenna design such as low cost, low profile, small sized, easy to fabricate, and antenna of multifunctional become one of the important demands in the modern era [1–4]. Also, in the wireless communication technology field, the performance of the wireless device needs to enhance in the domain of data and voice communication. The enhancement of different wireless device's performance concentrates on the lightweight, compact size, wider bandwidth for raise in data rate, etc. [5,6].

The antenna has unique characteristics like simple structure, small size, and wideband or multiband features. Therefore, antenna design plays a necessary part in wireless communication. The obtaining of an antenna with multi standard functions in a single antenna is a very decisive work for the antenna designers [7–9]. Growing the demands to develop the antennas in various applications has further intensified research studies in the wireless communication fields [10]. The wide traditional and complex wireless systems have been designed for many

different applications. These designs provide better performance with more reliable contacts. Hence, to achieve this goal, the wireless systems need to improve several parameters such as frequency band, radiation pattern, return loss, voltage standing wave ratio (VSWR), and gain [11]. Recently, microstrip antennas have gained tremendous research interest due to its lightweight, easily manufactured and high efficiency. Furthermore, the distinguished scientists developed several kinds of antennas such as microstrip patch, fractal, traveling wave, Yagi-Uda, slot, etc., for featured applications such as mobile communication, Bluetooth, infrared communication, Wi-Fi, satellite communication, ultra-wideband, etc. [12–15]. The applications of distinct wireless require various kinds of communication antennas. Hence, it is difficult for researchers to develop a new antenna without changing the performance of parameters. However, the fractal and microstrip antennas can offer the best findings due to its lightweight, compact size, simple structure, mechanically robust, economical fabrication, multiband, and wide bandwidth features [3,16]. The fractal geometry was inserted first time by Mandelbrot in 1975, this geometry fractal is repeating itself in a various iteration with a particular level [17,18]. Wide usage of fractals is due to the wideband and multiband features, space filling properties that help to achieve the size reduction and self-similarity. The available natural fractal shapes are feathers of peacock, broccoli, snowflakes, etc.

<sup>\*</sup> Corresponding author.

E-mail address: [raed.malallah@ucdconnect.ie](mailto:raed.malallah@ucdconnect.ie) (R. Malallah).

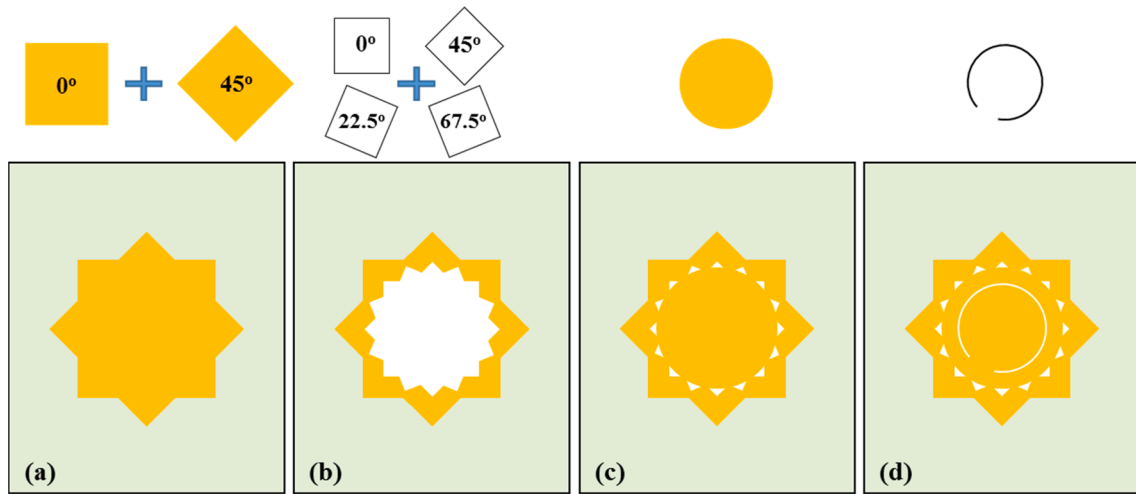


Fig. 1. Design development of the proposed antenna.

[19]. Fractal antennas are used in many fields such as medical, telecommunication, military, reduced size, array techniques, scattering problems, wide-band and multi-band antennas, and commercial applications [20,21]. Moreover, fractal and polar shapes of microstrip antennas are optimized for wireless sensors network applications [22].

In the recent years, many fractal antenna geometries for wireless applications have been suggested. Generally, the improvements in the performance of these antennas are referred to the self-similarity of fractals [23]. However, the fractal antenna shapes designs have emanated a revolution in the field of multiband antennas [24]. Many researchers have been proposed a several kinds of the fractal antenna geometries in the development field of multiband and wideband antennas [25]. Recursive procedures are used to generate the fractal shapes that produced a large surface region in bounded space [2,26]. Hence, the important factors to determine the resonant frequencies of the fractal antennas, are geometries and dimensions of these antennas [27]. The main characteristics in the fractal structures used to design the fractal antennas are space filling and self-similarity [19,28]. To achieve fractal antennas with multiband features, the multiple reduction copy machine algorithm can be used to obtain the self-similarity of fractal structures by applying the infinite number of iterations [29,30]. The size

antenna reduction can be achieved using the property of space filling. Also, an increase of the dielectric substrate properties like effective permittivity and permeability produce miniaturization antenna [31,32].

In this paper, innovative design for the star-shaped fractal antenna has been proposed to obtain the demands of multi-functional wireless applications. Thereby, an improved scheme was given to guarantee high efficiencies for the designed antenna. The suggested scheme was designed and simulated using an Ansoft® High Frequency Structure Simulator (HFSS) software. HFSS is a software package that is based on tow numerical methods, which are the finite element method and an integral equations (IEs) based on the method of moments (MoMs) technique.

## 2. Antenna configuration

The present manner depends on changing the shape of the patch antenna to improve the antenna performance. The proposed patch geometry is designed and fabricated using simple symmetry shapes such as squares and circles. Fig. 1 shows the design steps of the proposed antenna using HFSS software. Basic antenna geometry begins from two conducting equilateral square shapes to create an eight-shaped star, see

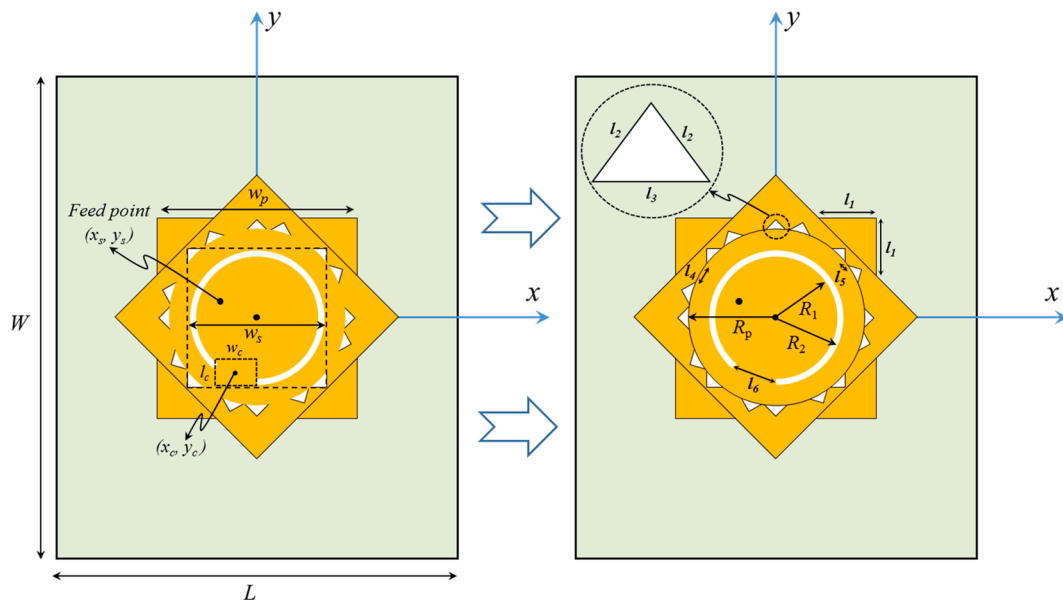


Fig. 2. Geometrical parameters of the designed antenna.

**Table 1**  
Dimensions of the optimum designed antenna.

Parameters	Dimensions (mm)	Parameters	Dimensions (mm)
$L$	100.00	$l_1$	15.23
$W$	112.00	$l_2$	3.78
$w_c$	12.00	$l_3$	5.35
$l_c$	11.00	$l_4$	4.99
$R_p$	22.00	$l_5$	2.23
$R_1$	16.00	$l_6$	11.86
$R_2$	15.75	$(x_s, y_s)$	(-6.00, -4.00)
$w_s$	34.66	$(x_c, y_c)$	(-6.00, -13.50)
$w_p$	52.00		

Fig. 1a. Similarly, the fractal geometry slot has been designed using squares rotating in four angles as shown in Fig. 1b. Fig. 1c shows the slot center which has been covered with a conducting circle to create sixteen triangular slots. Whereas semi-circle slot shaped has been loaded in the center of the proposed fractal antenna, see Fig. 1d.

The optimum geometrical dimensions of the proposed antenna are shown in Fig. 2. These parameters have been chosen carefully during the parametric study with return loss ( $S_{11}$ ) as a target provided by the HFSS software throughout changing the dimensions of the proposed antenna. It is also known that the acceptable resonance dimensions for designing any antenna are depended fundamentally on several reference values such as  $S_{11}$ , VSWR, gain, and directivity. In this paper, the optimum dimensions of the antenna designed have been taken to obtain the good qualitative agreement results of  $S_{11}$  and VSWR, to improve the proposed antenna performance. Table 1 lists all details of the parameter's

dimensions of the proposed antenna. As shown in the next sections, one of the merits of the suggested design is that several parameters can be varied to get the optimum results.

The antenna with optimum dimensions has been fabricated using a double-sided plain copper resist board (RS, AE16). The dielectric substrate is made from FR4-Epoxy with the dielectric constant of  $\epsilon_r = 4.4$  and a thickness of 1.6 mm. The total size of the ground plane of the fabricated antenna is  $100 \times 112 \text{ mm}^2$ . The length of both straight sides of the two conducting squares are  $w_p = 52 \text{ mm}$ . These conducting squares are rotated by two angles ( $0^\circ$  and  $45^\circ$ ). While the equilateral triangular slot dimensions are  $l_2 = 3.78 \text{ mm}$  and  $l_3 = 5.35 \text{ mm}$ .

As can be seen in Fig. 2, semi-circle slot have been created in the patch center with outer radius,  $R_1 = 16 \text{ mm}$  and inner radius  $R_2 = 15.75 \text{ mm}$ . While, the semi-circle cut length is  $l_6 = 11.86 \text{ mm}$  that was generated by rectangular shape sized ( $w_c \times l_c = 12 \times 11 \text{ mm}^2$ ), and located in (-6mm, -13.5 mm). The proposed antenna has been fed by a coaxial line. The feed location is selected at  $x_s = -6 \text{ mm}$  and  $y_s = -4 \text{ mm}$  to provide a good agreement impedance matching at  $50.0 \Omega$ .

### 3. Results and discussion

This study investigates the performance of the suggested antenna with the different parametric study. The software HFSS has been used to design and simulate the proposed antenna. The proposed antenna of the inscribed star-shaped fractal slot is shown in Fig. 2 with optimum dimensions as detailed in Table 1.

Fig. 3 shows the steps that have been taken to obtain the optimum shape of the final antenna designed to get good qualitative agreement

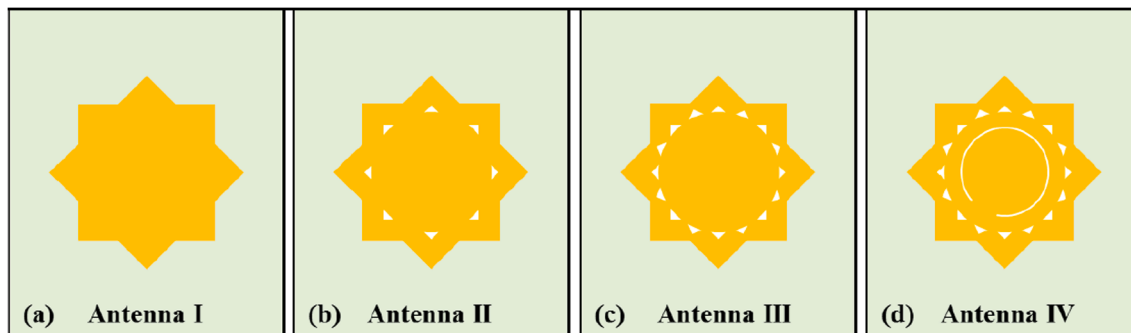


Fig. 3. Stapes selection of the suggested antenna.

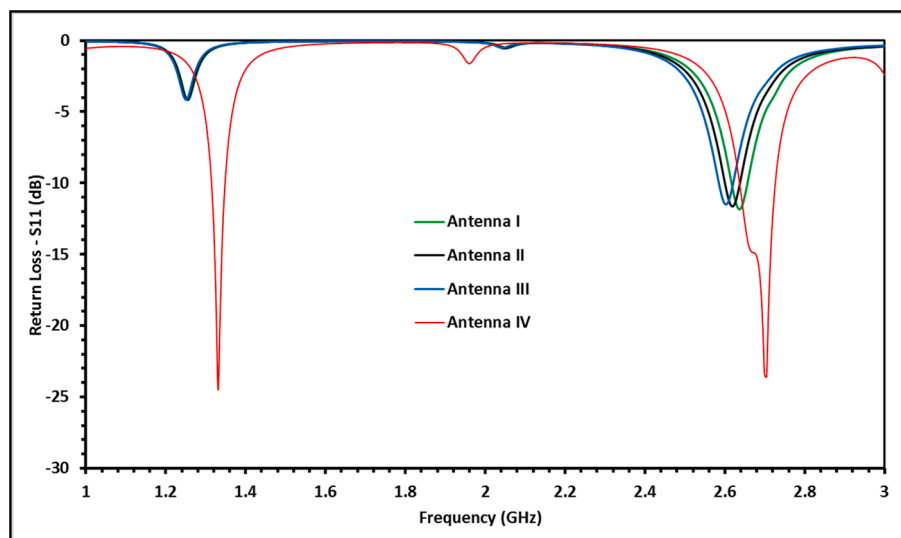


Fig. 4. Simulation results of return loss for the proposed antennas in Fig. 3.

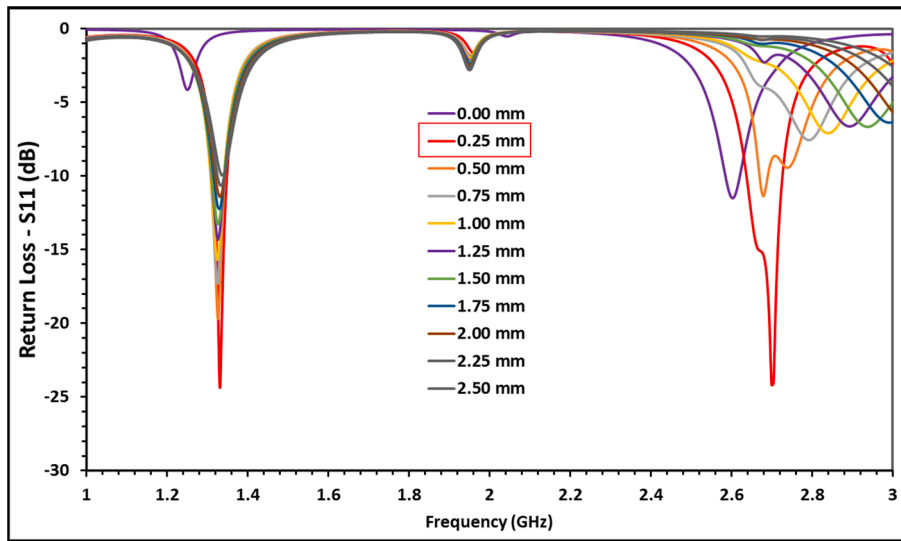


Fig. 5. Simulation results of  $S_{11}$  for proposed vs. semi-circle slot width ( $R_2-R_1$ ).

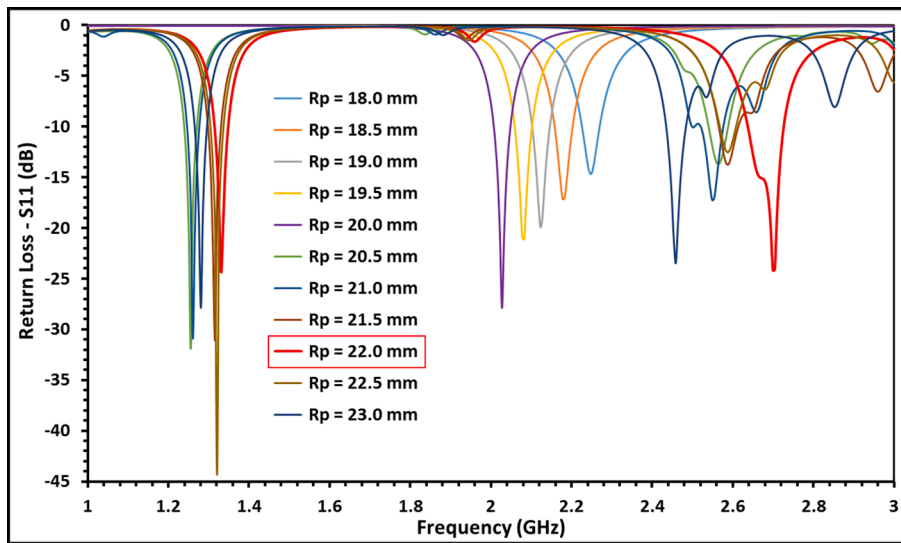


Fig. 6. Simulation results of  $S_{11}$  for proposed  $R_p$  values.

results. The first basic shape of the suggested antenna is shown in Fig. 3a. In the second step, eight and sixteen triangular holes were generated in the suggested patch, as shown in Fig. 1b and 1c, respectively. In the last step, the semi-circle slot shape has been etched on the proposed patch, see Fig. 3d.

The parametric study has been carried out on the return loss as a target for the various dimensions of the proposed antenna in order to enhancing its performance. Fig. 4 shows the simulation results of the return loss for the four models of the antenna in Fig. 3. In Fig. 4, the first three curves show one band with a little variation in the simulation results of the return loss of the first three design steps of the proposed antenna (Fig. 3a-c). While the fourth curves display dual band with appropriate return loss values in the simulation results of the return loss of the fourth design step (Fig. 3d). Dual bands have two resonant frequencies at 1.3308 GHz and 2.6992 GHz with return loss values  $-24.6$  dB and  $-23.9$  dB, respectively. However, the first three antennas designed have a single band at (2.6090, 2.6140 and 2.6441) GHz, sequentially. The explanation of these satisfactory simulation results of return loss is due to the high effect of the semi-circle slot on the antenna efficiency.

Based on the simulated result of the return loss of the proposed antenna in Fig. 3d, the designed antenna has a dual band due to etched semi-circle slot on the proposed patch. As can be seen from Fig. 2, the values of parameters  $R_1$  and  $R_2$  determine the thickness of the semi-circle slot.

Therefore, these parameters are changed sequentially to obtain different values of semi-circle slot thickness. In order to understand the effects of semi-circle slot thickness on the  $S_{11}$  result, several values of slot thickness have been presented in Fig. 5 by changing the value of  $R_2$  from 16.00 mm (without semi-circle slot) to 13.5 mm. This figure shows the simulation results of  $S_{11}$  for different values of semi-circle slot width. The best result of return loss can be obtained at semi-circle slot thickness value equal to 0.25 mm.

For more simulation studies, the triangular slots dimensions have been changed. These dimensions are basically depending on  $R_p$  value, see Fig. 2. The simulated results of  $S_{11}$  in Fig. 6 showed that the proposed antenna has one resonant frequency at  $R_p = 18.0$  mm to 20.0 mm and it has a dual band when  $R_p$  values between 20.5 mm and 23.0 mm. Moreover, the proposed antenna has an optimum result of  $S_{11}$  at  $R_p = 22$  mm with triangular slot dimensions are  $l_2 = 3.78$  mm and  $l_3 = 5.35$  mm.

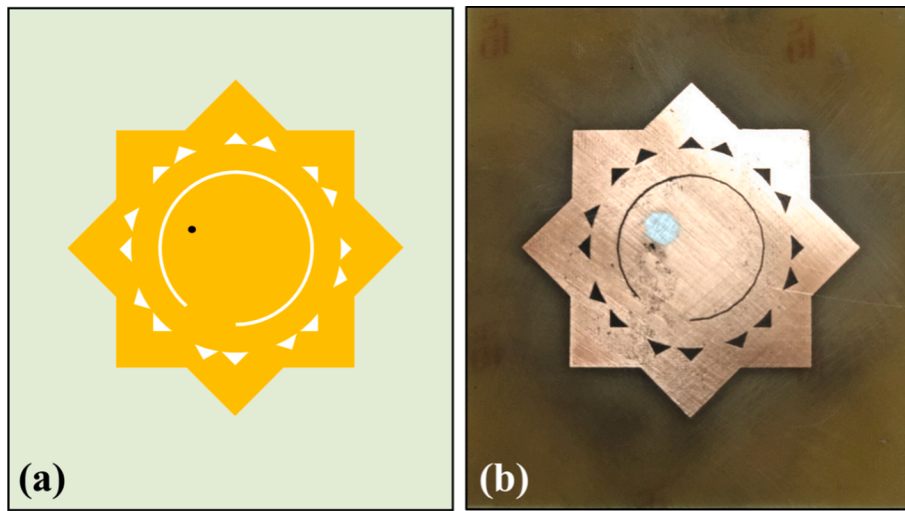


Fig. 7. Proposed antenna (a) antenna designed, (b) top view of fabricated antenna designed.

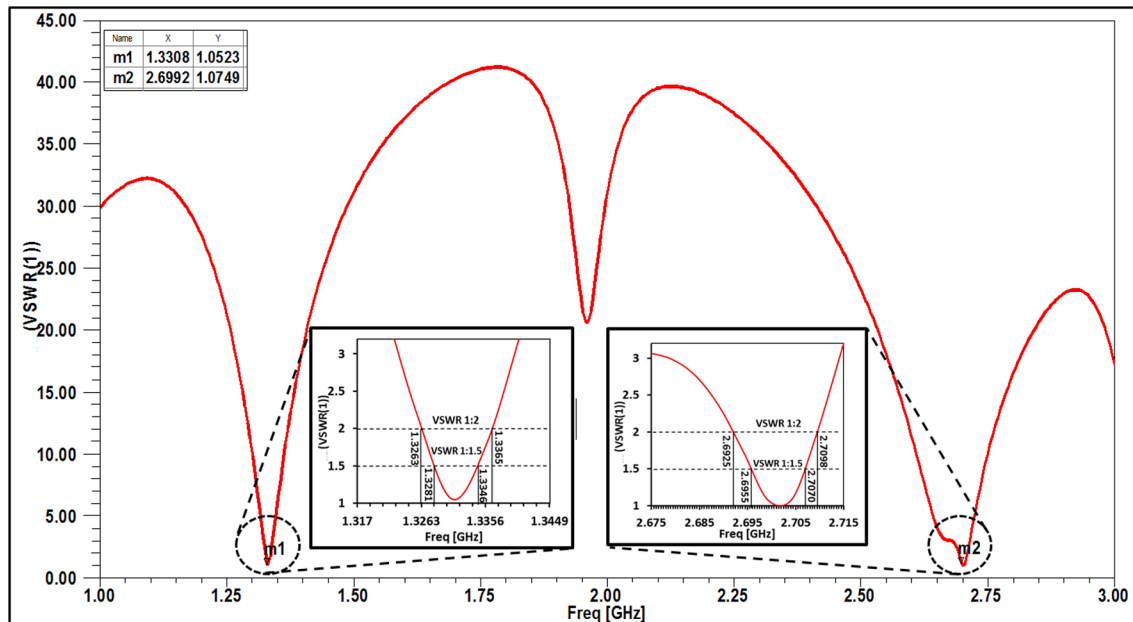


Fig. 8. VSWR simulation result of the optimum designed antenna in Fig. 7.

To validate the present results and the performance of the optimum antenna designed, the antenna designed has been fabricated using a double-sided plain copper resist board (RS, AE16). The substrate consists of a dielectric layer with a thickness 1.6 mm that is confined between two conductor layers, the dielectric constant is  $\epsilon_r = 4.4$ . Fig. 7 shows the geometrical shape and fabricated antenna the optimum design. Also, the dimensions and parameters used in designed and fabricated of the optimum antenna have been illustrated in Table 1.

Interestingly, the four equilateral squares in Fig. 1b are arranged geometrically to obtained angles with  $0^\circ$ ,  $18^\circ$ ,  $45^\circ$ , and  $63^\circ$  sequentially. This arrangement generates sixteen slots of triangular shapes which separated by  $l_4 = 4.99$  mm and  $l_5 = 2.23$  mm.

The VSWR characteristics of the proposed antenna have been simulated and studied. Fig. 8, shows the simulation results of VSWR for the antenna designed. This figure displays a dual band with two resonant frequencies 1.3308 GHz and 2.6992 GHz, these frequencies have corresponded to VSWR values of 1.0523 and 1.0749. Additionally, the frequency values at 1:1.5 and 1:2 of VSWR, for both bands, have been calculated as shown in Fig. 8. The first band shows the lower and upper

frequencies for both (1:1.5 and 1:2) VSWR rates, as (1.3281, 1.3263) GHz and (1.3346, 1.3365) GHz respectively. However, the lower and upper frequencies in the second band for both VSWR rates, have been calculated sequentially as (2.6955, 2.6925) GHz and (2.7070, 2.7098) GHz. It is worth noting that the second band has a large bandwidth compare with the first bandwidth.

Hence, the suggested antenna has a dual band which is located within L- and S-band respectively. Therefore, the proposed antenna meets the desired applications requirement in these two bands. These applications requirement including the military telemetry, GPS, mobile phones (GSM), and also especially in radar and satellite communications.

To proceed, we next explore and distinguish the actually achieved frequencies with its effect on the gain of the proposed antenna. The gain (dBi) vs frequency (GHz) plot for the optimum designed antenna is displayed in Fig. 9. This indicates that the proposed antenna performs well in both bands.

Experimental measurements have been performed to clarify the validity of the designed antenna using an antenna prototype, see Fig. 7b.

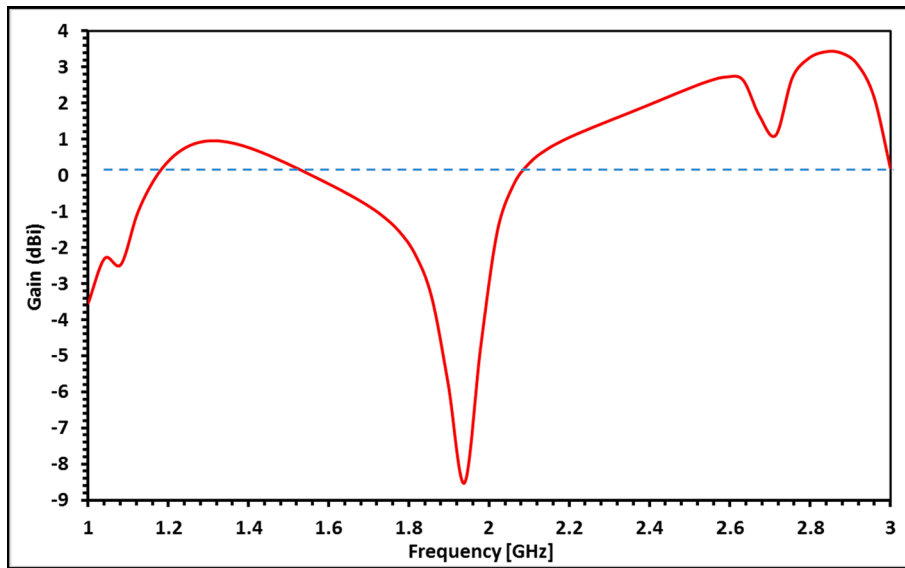


Fig. 9. Simulated peak gain (dBi) vs frequency (GHz) of the optimum designed antenna.

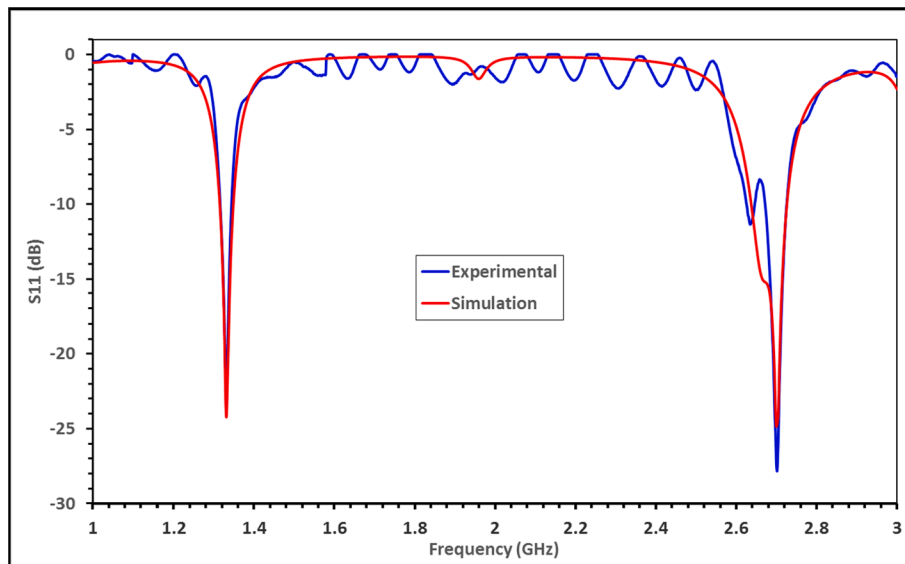


Fig. 10. Simulated and measured return loss features of the optimum designed antenna.

**Table 2**  
Simulated and measured return loss values of the optimum designed antenna.

Proposed antenna	Resonant frequency (GHz)	Return loss (dB)	Bandwidth (%)
Simulated	1.3308	-24.36	2.57
	2.6992	-24.18	3.32
Measured	1.3313	-22.88	2.31
	2.6997	-27.41	3.62

The comparison of the simulated and measured return loss features of the optimum designed antenna is found in good agreement especially within the two bands, as illustrates in Fig. 10. A little difference between the simulated and measured results may be caused due to the soldering effects used for the SMA connector, which is normally neglected in the simulation design.

Table 2 illustrates the fabricated antenna which has a dual band at resonant frequencies 1.3313 GHz and 2.6997 GHz with return loss values -22.88 dB and -27.41 dB, respectively. These measurement

findings of  $S_{11}$  are slightly different compared with the simulation findings. From Table 2, the measured values of the impedance bandwidth of the fabricated antenna are 2.31% and 3.62%. While the simulated values of the impedance bandwidth of the suggested antenna are 2.57% and 3.32%. These bandwidths are covering the roughly same mobile bands. In addition to that, these two bandwidths are extremely useful in L- and S- band applications.

The most important parameter when design an antenna is the feed impedance which is a control to transfer the power from source to the antenna. The simulation findings of the input impedance for the designed antenna as a function of frequency are illustrated in Fig. 11. This figure shows that the simulation values of input impedance in the two bands are close to  $50 \Omega$  which is the same standard impedance value of the coaxial feed line. These impedance values have been achieved by adjusting the optimum parameters of the proposed antenna and the coaxial feed location. Moreover, the simulated and measured impedance values at the two resonant frequencies are ( $49.61 \Omega$  and  $50.86 \Omega$ ) and ( $52.49 \Omega$  and  $51.87 \Omega$ ), respectively, see Table 3. A little difference between the simulated and measured findings of the input impedance

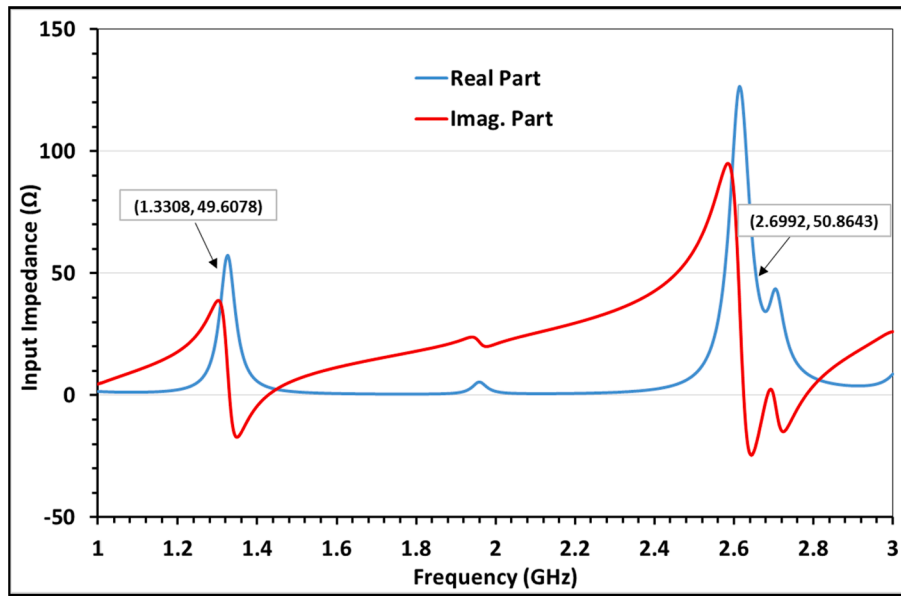


Fig. 11. Simulation results of the input impedance for the optimum designed antenna.

**Table 3**  
Simulated and measured values of input impedance for the optimum designed antenna.

Proposed antenna	Resonant frequency (GHz)	Real part of input impedance (Ω)
Simulated	1.3308	49.61
	2.6992	50.86
Measured	1.3313	52.49
	2.6997	51.87

and they are little higher than a standard value 50 Ω that is maybe due to the soldering effects used for the SMA connector.

Fig. 12 shows the simulation findings of the total gain (dBi) as a function of an azimuthal angle ( $\theta^\circ$ ) of the proposed antenna for both E- and H-planes. The value of the maximum total gain is 1.058 dBi. The results obtained in this figure at the two resonant frequencies have similar behavior to the other monopole antennas.

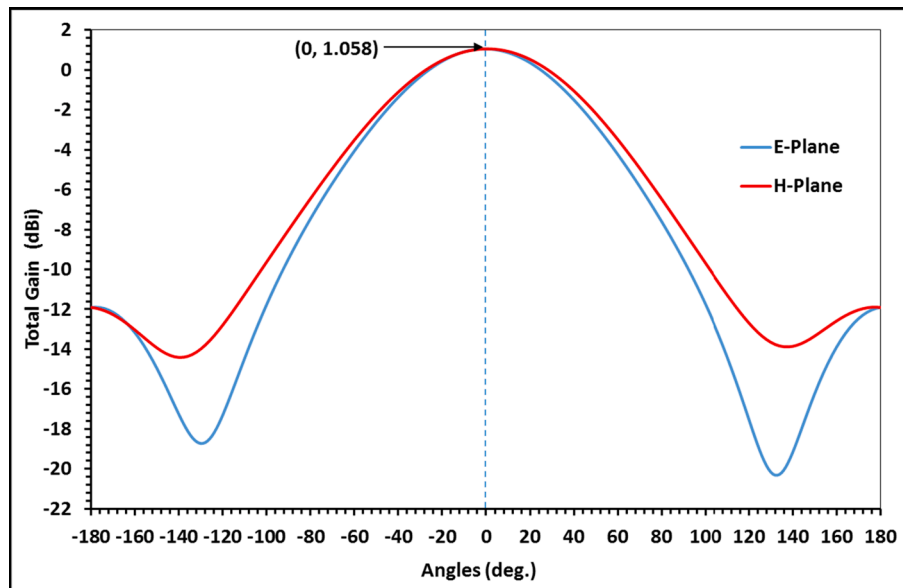


Fig. 12. Simulation findings of total gain (dBi) for the optimum designed antenna.

Fig. 13 illustrates the 2D- and 3D-radiation patterns of the proposed antenna at both resonant frequencies 1.3308 GHz and 2.6992 GHz. From this figure, the half power beamwidth in the E- and H-planes at the two resonant frequencies are (89° and 88°) and (96° and 86°), respectively. It can be noticed that Fig. 13 demonstrates the features of radiation patterns of the designed antenna, which are satisfactory in the wireless applications.

Fig. 14 shows the simulated results of co-polar and cross-polar radiation patterns of the optimum designed antenna. The proposed antenna is not symmetrical from the feed point, therefore the co-polar radiation patterns are not completely symmetrical, as shown in Fig. 13. It can be concluded that the small differences at the back lobe of the co-polar radiation patterns are due to the position of the feed in addition to the orientation of the semi-circle slot. The first and second bands of the proposed antenna can be achieved maximum cross-polarization of -15.54 dBi and -14.36 dBi in the angle -132° and -150° direction, respectively.



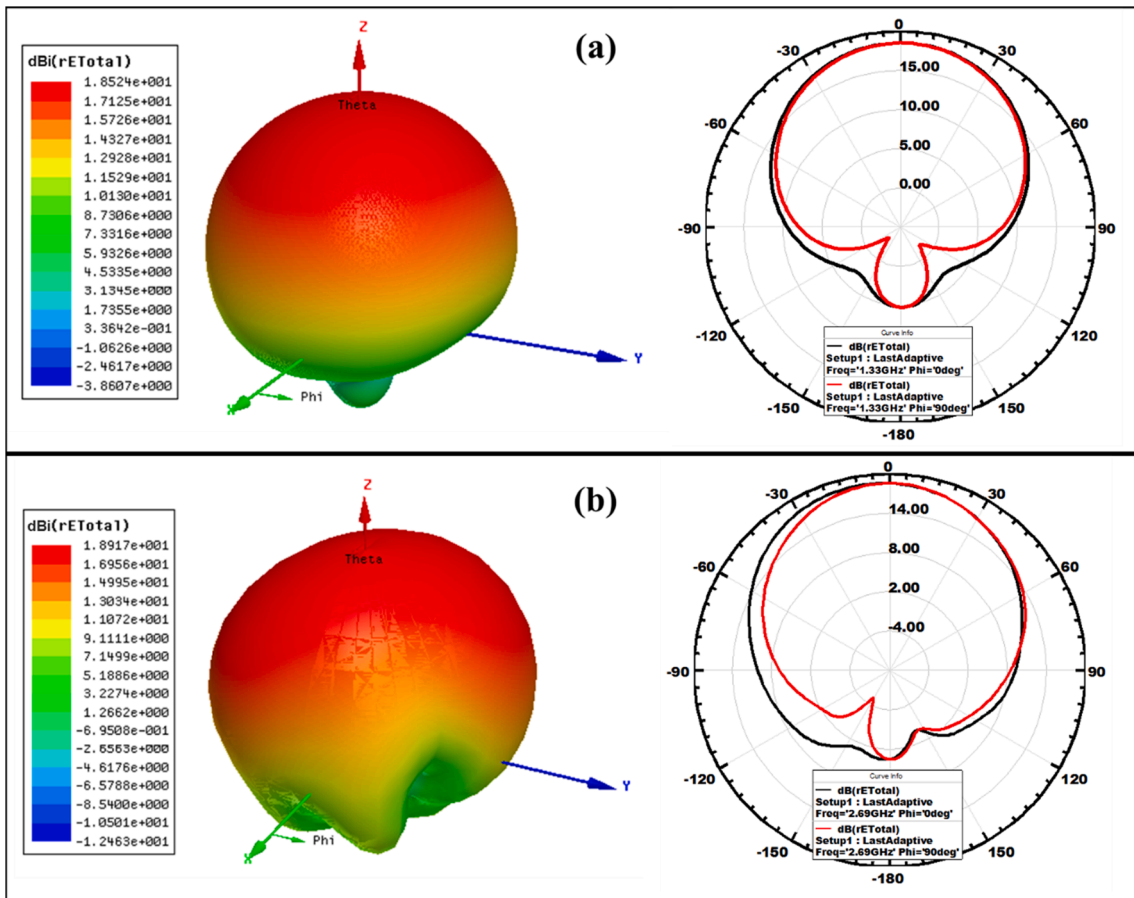


Fig. 13. Simulation findings of radiation pattern in 2D and 3D at both resonant frequencies: (a) 1.3308 GHz, and (b) 2.6992 GHz.

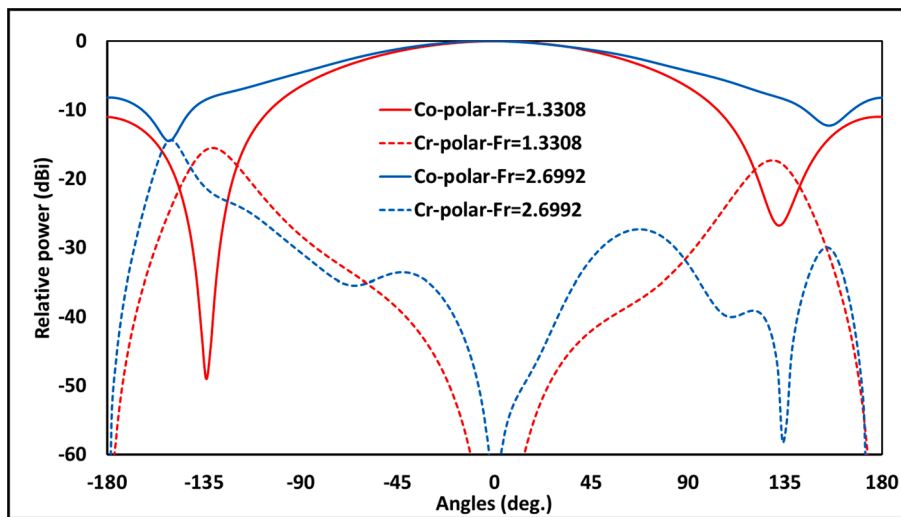


Fig. 14. Simulation findings of relative power for both co- and cross polar radiation pattern.

#### 4. Conclusions

Innovative design for the star-shaped fractal antenna has been proposed to obtain the demands of multi-functional wireless applications. The optimum parameters and dimensions of the designed antenna were used to fabricate it with size  $112 \times 100 \times 1.6 \text{ mm}^3$ . The features of the simulated and measured return loss of the designed antenna are in a good agreement. The semi-circle slot dimensions have a significant

effect on the simulation results of return loss and antenna efficiency. Moreover, etched semi-circle slot on the proposed patch produces a dual band antenna with two resonant frequencies 1.3308 GHz and 2.6992 GHz. These frequencies have corresponded to the VSWR values of 1.0523 and 1.0749. The measured and simulated values of the impedance bandwidth of the proposed antenna are (2.31% and 3.62%) and (2.57% and 3.32%), respectively. These bandwidths are covering the roughly same mobile bands. The proposed antenna meets the

applications in L- and S-band.

#### Author Contributions

Ra'ed Malallah and Raed Shaaban conceived of the presented idea, developed the simulation, fabrication and performed the computations. Ra'ed Malallah and Wa'il Al-Tumah discussed the results, wrote the manuscript and approved the final article.

#### Funding

This research did not receive any specific grant from funding agencies in the public, commercial, or not-for-profit sectors.

#### Declaration of Competing Interest

The authors declare that they have no known competing financial interests or personal relationships that could have appeared to influence the work reported in this paper.

#### Acknowledgements

Authors would like to express their gratitude towards the University of Basrah, College of Science, for their continuous support and encouragement during this work.

#### References

- [1] Oraizi H, Hedayati S. Microstrip slot antenna using the novel application of Giuseppe Peano fractal and CPW feed. In: The 8th European Conference on Antennas and Propagation (EuCAP 2014) 2014 Apr 6 (pp. 2063-2066). IEEE.
- [2] Sharma N, Sharma V. A journey of antenna from dipole to fractal: A review. *Journal of Engineering Technology*. 2017 Jul;6(2):317–51.
- [3] Sharma N, Bhatia SS. Performance enhancement of nested hexagonal ring-shaped compact multiband integrated wideband fractal antennas for wireless applications. *Int J RF Microwave Comput Aided Eng* 2020 Mar;30(3):e22079.
- [4] Al-Tumah WAG, Shaaban RM, Tahir A. Design, simulation and measurement of triple band annular ring microstrip antenna based on shape of crescent moon. *Int. J. Electron. Commun.* 2020;117(153133):1–8.
- [5] Khandelwal MK, Kanaujia BK, Dwari S, Kumar S, Gautam AK. Analysis and design of dual band compact stacked microstrip patch antenna with defected ground structure for WLAN/WiMax applications. *AEU-International journal of Electronics and Communications*. 2015 Jan 1;69(1):39–47.
- [6] Singh A, Singh S. A novel CPW-fed wideband printed monopole antenna with DGS. *AEU-International journal of Electronics and Communications*. 2015 Jan 1;69(1):299–306.
- [7] Al-Tumah WAG, Shaaban RM, Ahmed ZA. A modified E-shaped microstrip patch antenna for dual band in x- and ku-bands applications. *J. Phys. Conf. Ser.* 2019; 1234(1):012028.
- [8] Agrawal T, Srivastava S. Compact MIMO antenna for multiband mobile applications. *Journal of Microwaves, Optoelectronics and Electromagnetic Applications*. 2017 Apr;16(2):542–52.
- [9] Ullah S, Ruan C, Sadiq MS, Haq TU, He W. High Efficient and Ultra Wide Band Monopole Antenna for Microwave Imaging and Communication Applications. *Sensors*. 2020 Jan;20(1):115.
- [10] Yang HC, Alouini MS. *Advanced Wireless Transmission Technologies: Analysis and Design*. Cambridge University Press; 2020 Jan 30.
- [11] Najam AI, Duroc Y, Tedjini S. Multiple-input multiple-output antennas for ultra wideband communications. *Intech Open*. 2012 Oct;1(10):209–36.
- [12] Al-Tumah WAG, Shaaban RM, Tahir AS, Ahmed ZA. Multi-forked microstrip patch antenna for broadband application. *J. Phys. Conf. Ser.* 2019;1279(1):012025.
- [13] Parkash D, Khanna R. Design and development of CPW-fed microstrip antenna for WLAN/WiMAX applications. *Progress In Electromagnetics Research*. 2010;17: 17–27.
- [14] Bhatia SS, Sivia JS. A novel design of circular monopole antenna for wireless applications. *Wireless Pers Commun* 2016 Dec 1;91(3):1153–61.
- [15] Shaaban RM, Ahmed ZA, Godaymi WA. Design and analysis for circular microstrip antenna loaded by two annular rings. *Glob. J. Comput. Sci. Technol.* 2017;17(1): 31–5.
- [16] Sharma N, Sharma V, Bhatia SS. A novel hybrid fractal antenna for wireless applications. *Progress In Electromagnetics Research*. 2018;73:25–35.
- [17] Oraizi H, Hedayati S. Miniaturization of microstrip antennas by the novel application of Giuseppe Peano Fractal Geometries. *IEEE Trans Antennas Propag* 2012;60(8):3559–67.
- [18] Reddy VV, Sarma NVSN. Compact circularly polarized asymmetrical fractal boundary microstrip antenna for wireless applications. *IEEE Antennas Wirel Propag Lett* 2014;13:118–21. <https://doi.org/10.1109/LAWP.2013.2296951>.
- [19] Sharma N, Bhatia SS. Split ring resonator based multiband hybrid fractal antennas for wireless applications. *AEU-International Journal of Electronics and Communications*. 2018 Sep;1(93):39–52.
- [20] Sivia JS, Bhatia SS. Design of fractal based microstrip rectangular patch antenna for multiband applications. In: 2015 IEEE International Advance Computing Conference (IACC) 2015 Jun 12 (pp. 712-715). IEEE.
- [21] Bangi IS, Sivia JS. Minkowski and Hilbert curves based hybrid fractal antenna for wireless applications. *AEU-International journal of Electronics and Communications*. 2018 Feb;1(85):159–68.
- [22] Da Silva Junior PF, Silva Filho MS, de Carvalho Santana EE, da Fonseca Silva PH, de Oliveira EE, de Oliveira MA, Batista FF, Serres AJ, Freire RC, Souza A, Neto S. Fractal and polar microstrip antennas and arrays for wireless communications. In: *Wireless Mesh Networks-Security, Architectures and Protocols* 2019 Oct 23. IntechOpen.
- [23] Krzysztofik WJ, Brambila F. Fractals in antennas and metamaterials applications. In: *Fractal Analysis: Applications in Physics, Engineering and Technology* 2017 Jun 14 (pp. 953-978). InTech.
- [24] Azaro R, Debiase L, Zeni E, Benedetti M, Rocca P, Massa A. A hybrid prefractal three-band antenna for multistandard mobile wireless applications. *IEEE Antennas Wirel Propag Lett* 2009 Jul;28(8):905–8.
- [25] Behera S, Vinoy KJ. Multi-port network approach for the analysis of dual band fractal microstrip antennas. *IEEE Trans Antennas Propag* 2012 Jul 11;60(11): 5100–6.
- [26] Bhatia SS, Sivia JS, Sharma N. An optimal design of fractal antenna with modified ground structure for wideband applications. *Wireless Pers Commun* 2018 Dec 1; 103(3):1977–91.
- [27] Puente-Baliarda C, Romeu J, Pous R, Cardama A. On the behavior of the Sierpinski multiband fractal antenna. *IEEE Trans Antennas Propag* 1998 Apr;46(4):517–24.
- [28] Brambila F, editor. *Fractal Analysis: Applications in Physics, Engineering and Technology*. BoD–Books on Demand; 2017 Jun 14.
- [29] Choukiker YK, Sharma SK, Behera SK. Hybrid fractal shape planar monopole antenna covering multiband wireless communications with MIMO implementation for handheld mobile devices. *IEEE Trans Antennas Propag* 2013 Dec 17;62(3): 1483–8.
- [30] Gianvittorio JP, Rahmat-Samii Y. Fractal antennas: A novel antenna miniaturization technique, and applications. *IEEE Antennas Propag Mag* 2002 Aug 7;44(1):20–36.
- [31] Oraizi H, Soleimani H. Miniaturization of the triangular patch antenna by the novel dual-reverse-arrow fractal. *IET Microwaves Antennas Propag* 2014 Dec 12;9(7): 627–33.
- [32] Mitra D, Ghosh B, Sarkhel A, Chaudhuri SR. A miniaturized ring slot antenna design with enhanced radiation characteristics. *IEEE Trans Antennas Propag* 2015 Nov 2;64(1):300–5.